First publ. in: Physical Review B 80 (2009), 014402

# Quasiantiferromagnetic 120° Néel state in two-dimensional clusters of dipole-quadrupole-interacting particles on a hexagonal lattice

N. Mikuszeit,[1,*] L. Baraban,[2] E. Y. Vedmedenko,[1] A. Erbe,[2] P. Leiderer,[2] and R. Wiesendanger[1]
[1]*Institute of Applied Physics, University of Hamburg, Jungiusstr. 11, 20355 Hamburg, Germany*
[2]*Department of Physics, University of Konstanz, Universitätsstr. 10, Konstanz 78457, Germany*

The magnetostatic interactions of colloidal particles, "capped" with radially magnetized Co/Pt multilayers, are modeled. Motivated by experiment the particles are arranged in microscopic two-dimensional clusters on a hexagonal lattice and are free to rotate. The thermodynamically stable states of clusters containing up to 108 particles are calculated theoretically by means of Monte Carlo simulations in the framework of multipole expansion. It is shown analytically that radially magnetized hemispheres have higher-order multipole moments beyond the dipole. Depending on geometrical details also even order moments appear. The even order moments break the inversion symmetry of the magnetic potential of a single particle. For a specific mixing ratio of dipole and quadrupole moments, the experimentally observed antiferromagnetic 120° Néel state in the clusters is found.

PACS number(s): 41.20.Gz, 75.10.−b, 75.50.Mm, 47.57.J−

## I. INTRODUCTION

Recent experiments on colloidal clusters, consisting of particles that are covered by Co/Pt multilayers,[1] have shown a 120° Néel state that was unexpected for particles with magnetic moments interacting via stray field. In particular, this structure cannot be understood by only taking dipole moments into account. When describing the stray field interaction in the framework of multipole moments and multipole-multipole interaction, the 120° Néel state requires the consideration of higher-order moments. As each order of multipole moments has a different lattice-dependent ground-state symmetry, mixing different orders gives rise to competing interaction and complex structure formation.[2]

Even if for a single type of interaction the pair interaction is well understood, the ground state of a large system may not be clear intuitively. An example is the simple quadrupole-quadrupole interaction of linear quadrupoles, e.g., hydrogen molecules.[3] The pair interaction prefers orthogonal orientation. This relative orientation can be realized in linear chains or two-dimensional (2D) square (rectangular) lattices. However, this configuration is frustrated on a 2D hexagonal lattice and the ground state is the complicated pinwheel structure.[4,5] If the quadrupole is forced in plane, a herringbone structure is formed.[6]

On the other hand the linear quadrupole still is simple in the sense that it has inversion symmetry. Not necessarily but very often also the ground state shows inversion symmetry if the single particle and the underlying lattice show inversion symmetry.[7–9]

Breaking inversion symmetry of the single-particle potential makes things more complicated. If the interaction can be described by long-range multipole moment interaction,[10] the lowest-order possibility of breaking inversion symmetry in finite systems is the combination of monopole and dipole. However, a nonvanishing monopole would result in an infinite energy in an infinite system. Therefore, this combination is forbidden in the thermodynamic limit and the first nontrivial combination is the dipole-quadrupole system occurring, e.g., in $H_2O$ or $H_3N$ molecules.[11,12]

A quadrupolar contribution to the dipole-dipole interaction has interesting effects. While a pure dipolar system on an infinite square lattice has a degenerate ground state, a small quadrupole moment lifts the degeneracy and introduces an energy gap for the low-energy excitations.[13] In clusters of particles that are free to move in three dimensions, the quadrupole moment destroys planar configurations and leads to three-dimensional clusters.[14]

It will be shown in the following that the noncollinear 120° Néel state, recently found in systems of colloidal particles,[1] can be attributed to a quadrupole moment that breaks the symmetry of the presumably dominant dipole moment. The inversion symmetry of the pure dipole is broken and the resulting ground state—the 120° Néel state—also does not exhibit inversion symmetry.

After shortly summarizing the experiments and the experimental results (Sec. II) the theoretical tools will be presented in Sec. III. A simple model of the magnetic cap justifying the existence of a quadrupole moment is introduced and the Monte Carlo method, utilized to find the thermodynamically stable states, is explained. The results are presented and discussed in Sec. IV.

## II. EXPERIMENT

Magnetic colloidal clusters of so-called "capped" colloidal particles with artificially designed magnetic moments were formed by aggregation in water solution. In order to produce the capped colloidal particles, a closely packed monolayer of silica spheres (diameter $d$=4.75 $\mu$m) was formed on a glass substrate; the self-organization of colloidal particles in arrays with hexagonal symmetry has, e.g., been used as a deposition mask for nanostructure formation and for soft lithography.[15] The magnetic moment of the spheres was provided by deposition of the multilayer stack Pt(1 nm)/[Co(0.3 nm)/Pt(0.8 nm)]$_8$/Pt(5 nm) onto a self-assembled monolayer of particles [Fig. 1(a)], as has been described elsewhere.[1,16] The Pt/Co multilayer exhibits out-of-plane magnetic anisotropy. Deposition of the metallic

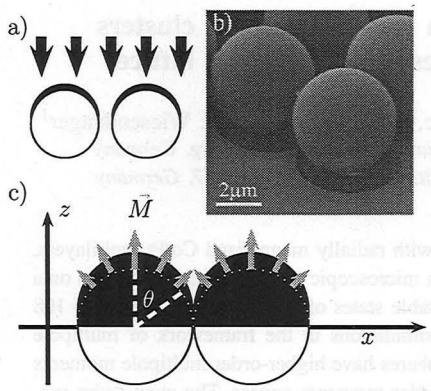


FIG. 1. (Color online) Properties of the capped particles. (a) Metallic layers are deposited on top of silica spheres by thermal evaporation and molecular beam epitaxy; (b) scanning electron microscope (SEM) image illustrates capped colloids—particles with metallic hemispheres (green) on top; and (c) sketch of capped particles in the parallel orientation that is used to normalize the interaction energy. The direction of magnetization stays normal to the surface of the metal film.

films on the surface of the spheres leads to the formation of hemispherical metallic "caps" on every particle as displayed in the SEM image [Fig. 1(b)]. The multilayer of Co/Pt exhibits strong magnetic anisotropy perpendicular to the plane of the film following the spherical shape of the particle. In addition, reduction in the thickness of magnetic films from the top of the sphere toward the equator causes the decay of the magnetization along the particle's surface[16] [Fig. 1(c)]. An external magnetic field was applied to saturate the particles in the $z$ direction, thus assuring equivalent magnetic states and magnetic moments for all spheres. To suspend the particles in distilled water they were detached from the glass substrate using an ultrasonic bath. The colloidal suspension was placed in a measurement cell for carrying out the experiments. The metallic capping introduces a strong optical inhomogeneity that allows visualization of the magnetic arrangement and growth of clusters via video microscopy. The good optical resolution allows the determination of the orientations of the magnetic caps (see Fig. 2 and inset of Fig. 5). Hence, as the magnetic moments of the silica particles coincide with the axis of the capping, the orientations of the magnetic moments can be measured solely by this optical method. The growth of the clusters was carried out by gradual addition of the particles using laser tweezers.[1,17] It should be noted that every single colloidal particle, attached to the cluster, was free to move and free to rotate in order to find the state corresponding to the minimum energy. Thus, it was demonstrated that grouping of the capped colloids leads to the formation of a series of the *magic* clusters,[1,18] stabilized by the noncollinear quasiantiferromagnetic order.[19] These clusters (see Fig. 2) were found to be purely two dimensional, meaning that all colloidal particles were arranged in a single layer and all macrospins of the particles lied strictly in the plane that is coplanar to the substrate. The arrangement of the magnetic moments in clusters, shown in Fig. 2, is consistent with the 120° Néel state for spin lattices with triangular symmetry.[19]

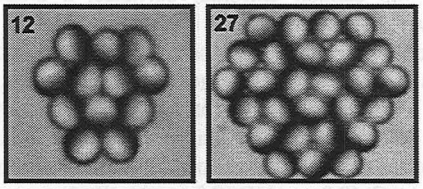


FIG. 2. Magnetic colloidal clusters with 2D arrangements of macrospins, which resemble a 120° Néel state, observed for antiferromagnets on triangular lattices.

## III. THEORETICAL TOOLS

The thermodynamically stable states of the clusters are calculated theoretically by means of Monte Carlo simulations in the framework of multipole expansion. In order to estimate the contribution of the multipole components, the moments of an ideal dipole cap were calculated. The reference energy scale is chosen as the pair interaction $E_{\uparrow\uparrow}$ of two spheres, both pointing in the $z$ direction ($\uparrow\uparrow$) and separated by a unit distance $\hat{u}$ in the $x$ direction (see Fig. 1). This choice is somewhat arbitrary, but it can be extended from pair interaction to the whole cluster, whereas, e.g., a head-to-head configuration ($\rightarrow\leftarrow$) would be frustrated. The highest pair interaction energy is given by the head-to-head configuration, while the lowest energy depends on geometrical and magnetic details of the cap. To compare results for caps with different properties, the energies are normalized in such a way that the pair interaction $E_{\uparrow\uparrow}$ of two spheres, both pointing in the $z$ direction and separated by a unit distance in the $x$ direction ($\uparrow\uparrow$), defines one energy unit. The diameter of the spheres is $1\hat{u}$.

### A. Calculating the multipole moments

To calculate the multipole moments we use spherical coordinates. The coordinate system is chosen in such a way that the $z$ direction is the symmetry axis of the cap, which is assumed to have rotational symmetry. Although the spheres are magnetic the moments are defined via charge, i.e., we define a magnetic surface charge $\sigma$,

$$\sigma(\vec{r}) = \mu_0 \vec{n}(\vec{r}) \cdot \vec{M}(\vec{r}), \tag{1}$$

where $\vec{n}$ is the outward surface normal of the cap. Hence, we are not using vector spherical harmonics; all steps are equivalent to electric charge—except that the total charge must be zero. The moments are given by the surface integral

$$Q_{lm} = \int_S dS \sigma(\vec{r}) R_{lm}(\vec{r}), \tag{2}$$

where $R_{lm}$ is the regular normalized solid spherical harmonic.[20] It is known from micromagnetic simulations that the magnetization vector field is radially pointing outward,[21] which would give a constant surface charge. As the cap has a very small thickness, the volume charge

$$\varrho(\vec{r}) = -\mu_0 \vec{\nabla} \cdot \vec{M}(\vec{r}) \tag{3}$$

is neglected. Furthermore, the thickness is decreasing when going to the edges of the magnetic cap. As an approximation we take the latter effect into account by decreasing $\sigma$ proportional to cos $\theta$ (see Fig. 1) toward the edge. As the thickness $d$ of the cap is small compared to its radius, we make the typical dipole limits $d \to 0$ and $\sigma \to \infty$, which allow us to express the results in terms of the cap's total saturation moment $\mu_0 M_S V$, where $V$ is the cap volume. Hence, this moment is different from the cap's dipole moment $Q_{10}$ as the cap is not homogeneously magnetized. The dipole limit approximates an infinitely thin dipole layer with decreasing dipole strength toward the equator proportional to the cosine.

In contrast to standard conventions, we chose the center of the sphere as origin, although it is not the center of charge. This simplifies the simulation as otherwise a rotation of a sphere not only changes the orientation of the multipoles but also their position in space. It would also be possible to calculate the multipole moments in a coordinate system where origin and center of charge coincide. Afterward the moments can be transformed by a change of origin. The general transformation of multipole moments upon a change of origin by a vector $\vec{x}$ has the form[20]

$$\frac{(-1)^{L+M} Q_{LM}^{\text{new}}}{\sqrt{(2L+1)!}} = \sum_{\substack{l+\lambda=L \\ m+\mu=M}} \frac{Q_{lm}^{\text{old}} R_{\lambda\mu}(\vec{x})}{\sqrt{(2l)!\,(2\lambda)!}} \begin{pmatrix} l & \lambda & L \\ m & \mu & -M \end{pmatrix}, \tag{4}$$

where the expression in the last parentheses is the Wigner $3j$ symbol.[22] Note that all orders $l \leq L$ contribute to the transformed moment $Q_{LM}$. The dipole, as well as the quadrupole, contributes to an octopole (and higher orders) in the shifted system and the calculation of interaction energy might require higher-order moments. As it is estimated that the octopole and higher moments are small when choosing the center of a sphere as origin (see Appendix), this choice does not only simplify the simulation by keeping the intermoment distances constant but also reduces the required order of expansion.

Due to the rotational symmetry only $Q_{lm}$ with $m=0$ can be different from zero. The moments have the form

$$Q_{l0} = \mu_0 M_S V A_l(\theta_c) r_S^{l-1} l, \tag{5}$$

where $r_S$ is the radius of the sphere. The coefficients $A_l(\theta_c)$ are given in Appendix. As the thickness of the cap decreases toward the edge, the angle $\theta_c$ takes into account that the cap may only be magnetic up to this critical angle. In this approximation of $Q_{lm}$ the main contribution to energy is the dipole-dipole interaction, but the quadrupole has a strong influence. Higher-order components are important for proper visualization of the magnetic potential $\Phi(\vec{r})$, which fulfills $-\vec{\nabla}\Phi(\vec{r}) = \vec{H}(\vec{r})$ (see Fig. 3), but they contribute only little to the total energy if $\theta_c > \pi/3$.

In conclusion, in the natural system of the sphere, the two most important energy contributions are due to dipole and quadrupole.

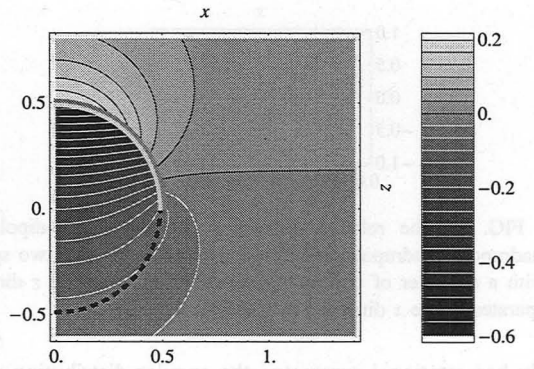


FIG. 3. (Color online) Contour plot in the $x$-$z$ plane of the magnetic potential $\Phi$ (with arbitrary scaling) of a cap with $\theta_c = \pi/2$ and $\sigma \propto \cos\theta$. Negative equipotential lines are white, while constant $\Phi \geq 0$ A are shown in black. The potential is evaluated from the multipoles up to order 32. The contour line with $\Phi = 0$ A—the almost horizontal one in the right-hand side of the figure—is shifted in direction of larger $z$ if $\theta_c$ decreases. The dipole cap is indicated by a red-green double line.

### B. Monte Carlo simulation

The thermodynamically stable states are found via Monte Carlo simulations. The code accepts multipole moments up to arbitrarily high order as well as any combination of moments. The interaction is calculated without cutoff, i.e., even for high orders the full long-range character of the interaction is taken into account. The utilized code is a standard Metropolis algorithm, accepting each new state with probability $p=1$, if it has lower energy than before, and with $p = \exp[-\beta\Delta E]$, if its energy is higher by $\Delta E$. The starting temperature $T_{\text{start}}$ is chosen such that $k_B T_{\text{start}} = \beta_{\text{start}}^{-1} > 2E_{\uparrow\uparrow}$. The final temperature fulfills $\beta_{\text{final}}^{-1} < 5 \times 10^{-3} E_{\uparrow\uparrow}$. The high temperature is sufficient to destroy any ordered state while the system freezes for the low temperature. The decrease in temperature is performed in at least $10^3$ steps in such a way that the number of steps per temperature decade is constant. For each temperature several $10^3$ Monte Carlo steps were performed. Consequently, the number of performed steps for one cooling procedure was larger than $10^6$.

In experiment the particles are to some extent free to move but form a densely packed 2D cluster, i.e., a hexagonal structure. Therefore, we perform the simulation with fixed particle position on a perfect hexagonal lattice, but the spheres and therefore the multipole moments are allowed to rotate freely on their lattice sites.

Theoretically, it is possible to calculate the moments up to any desired order assuming the dipole cap with cosine-decreasing charge density. It is, however, doubtful that the high moments describe the real experimental system. The model is too idealized to describe the moments quantitatively. Qualitatively, it shows that the main contribution to the interaction of the spheres should be due to the dipole and the quadrupole moments. Therefore, we restrict the simulations to these lowest orders. In detail the strength of the dipole compared to the quadrupole depends on several unknown parameters: the critical angle $\theta_c$, whether the cap re-

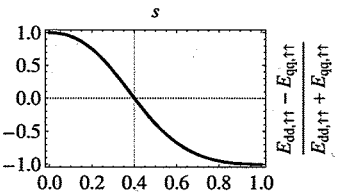


FIG. 4. The relative difference between dipole-dipole and quadrupole-quadrupole energies as a function of $s$ for two spheres (with a diameter of one unit distance) pointing in the $z$ direction separated in the $x$ direction by one unit distance.

ally has rotational symmetry, the angular distribution of the magnetization vector field, i.e., if the magnetization is radially aligned, etc. To take this uncertainty into account, we have tested several combinations of dipole-quadrupole strengths. When comparing the strength of dipole and quadrupole, we refer to the energy of the dipole-dipole and the quadrupole-quadrupole interactions in the above mentioned $\uparrow\uparrow$ configuration. To combine the moments we use the continuous parameter $s \in [0,1]$ and construct the dipole and quadrupole moments as

$$Q_{10} = \frac{(1-s)\hat{D}}{\sqrt{1-2s+\frac{13}{4}s^2}}, \quad Q_{20} = \frac{s\hat{D}\hat{u}}{\sqrt{1-2s+\frac{13}{4}s^2}}, \tag{6}$$

where $\hat{D}$ is a unit dipole moment and $\hat{u}$ is the aforementioned unit distance. The parameter space is confined by the pure cases, pure dipole ($s=0$), and pure quadrupole ($s=1$). The denominator is a normalization. In Fig. 4 it is shown how the relative energy contribution changes from dipole-dipole to quadrupole-quadrupole energy as a function of $s$. For $s=0.4$ both energy contributions are identical.

### C. Insight derived from symmetry

Apart from the analytic results for the multipole moments, the experimental observation clearly justifies the appearance of even order moments in addition to the odd order dipole. Looking at the symmetry of the experimentally found ground state, it is clear that the interaction is not purely dipolar. First, the particles are grouped together manually forming a hexagonal arrangement. The dipolar ground state at $T=0$ K in an infinite hexagonal lattice is quasiferromagnetic, i.e., all dipoles align in one direction.[8] In a finite sample usually a vortex is formed. Second, the odd parity of a dipole would give the same energy to the ground state if all dipoles are reversed. Obviously, this would change the experimentally found images. The energy of the reversed state is probably higher and, therefore, not observed. The explanation via the parity of the dipole also holds for combinations of moments of higher order if all have the same parity. The observed symmetry cannot be explained by combining dipole, octopole, and higher-order odd moments. These moments would increase the tendency to form a collinear state and a vortex would become less favorable.[23] If all moments would have even parity again the reversed state would have the same energy. Therefore, it is clear that a combination of even and odd moments is required.

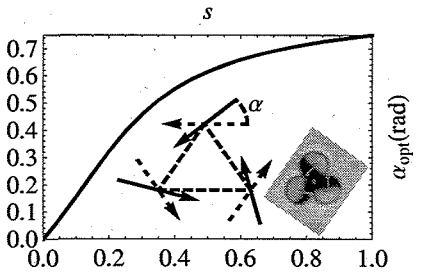


FIG. 5. (Color online) Optimal angle $\alpha$ (see text) for a three-particle cluster as a function of quadrupole contribution $s$. The pure dipole case (solid arrows) corresponds to $\alpha=0$ rad.

## IV. RESULTS AND DISCUSSION

The smallest nontrivial cluster consists of three particles on a triangle. In this case always a vortex is formed but the angle between the magnetic moments changes with $s$. In case of the pure dipole the dipole vector is a tangent to the circumcircle of the triangle, i.e., it is parallel to the opposite edge and has a 60° angle to the distance vector to its neighbor (see inset of Fig. 5). This high-symmetry state does not change energy if all dipoles are reversed; it has the lowest stray field. In contrast to this the stray field is not important for the quadrupole, as quadrupoles interact with the field gradient. Furthermore, the lowest pair interaction is achieved if two neighboring axial quadrupoles (type $Q_{20}$) form the so-called T structure, i.e., one is parallel and the other one is perpendicular to the distance vector. Therefore, with increasing quadrupole contribution the dipoles turn inward by an angle $\alpha$. The optimal angle $\alpha_{opt}$ that minimizes the energy as a function of $s$ is shown in Fig. 5. Both, dipole and quadrupole, are frustrated on a triangle and cannot reach their lowest possible pair interaction. However, the pure quadrupole almost reaches its 90° T configuration and turns by $\alpha_{s=1} = \arccos\sqrt{15/28} \approx 0.75 = 43°$ out of the position of the pure dipole. Hence, the angle to its neighbor is 86°. Although it is difficult to extract precisely the turning angle from the experimental pictures of a three-particle cluster, it is roughly estimated to be $30° \pm 5°$, which corresponds to $0.27 < s < 0.5$. This includes the values that give the Néel-type structure in larger clusters.

The low energy states for a symmetric 12-particle cluster for different $s$ are shown in Fig. 6. This cluster type is also studied experimentally (see Fig. 2). The pure dipolar case forms the expected vortex. Increasing the quadrupole contribution the vortex state is destabilized. There are two typical low energy orientations for a pair of dipoles. The lowest energy is achieved by parallel dipoles with a distance vector parallel to the dipole vector ($\rightarrow\rightarrow$). The lowest energy for antiparallel alignment is achieved if the distance vector is perpendicular to the dipole vector ($\uparrow\downarrow$). The quadrupole increases the energy of both configurations. Hence, the quadrupole suppressed the collinear states of the dipole. For $s$

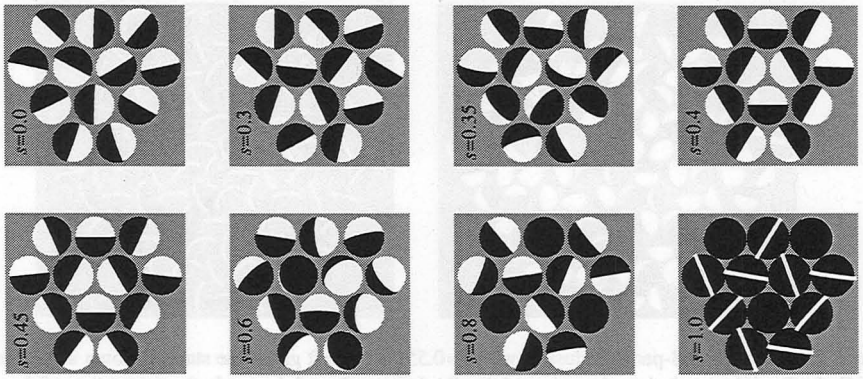


FIG. 6. Monte Carlo simulations of 12-particle clusters and varying quadrupole contribution. The dipolar state ($s=0$) shows the typical vortex state. In case of the pure quadrupole ($s=1$) the equatorial plane is plotted as the parity is even and the up and down directions are degenerate. Hence, in this case it does not make sense to interpret the black caps as magnetic material. The cluster represents a section of the well-known pinwheel structure (Refs. 4 and 5). For intermediate $s$ the 120° Néel structure appears similar to the ground state observed in experiments.

$=0.3$ the dipole contribution still forces the formation of a vortex, but the influence of the quadrupole is already visible. In a simplified way this influence can be described as a tendency to form a zigzag, as all quadrupole dominated configurations show some characteristics of a herringbone structure. One example is the herringbone ground state of $xy$-quadrupolar systems on a hexagonal lattice as mentioned in Sec. I. In case of the $3d$-pinwheel state the zigzag forms along an in-plane row (see Fig. 7). Within the Néel state it is visible when removing one sublattice.

Between $s=0.35$ and $s=0.5$ the Néel-type state is observed. As can be seen from Fig. 4, at $0.35 \lesssim s \lesssim 0.45$ the dipole-dipole and quadrupole-quadrupole interactions contribute almost identically to the energy. For $s=0.45$ the vortex configuration is energetically not preferred anymore. To show this quantitatively, we forced particles with $s=0.45$ into the solution found for a 12-particle cluster and $s=0.0$. The energy of the forced states has been evaluated to be $E_{\text{vortex}}^{\text{forced}} = -1.60E_{\uparrow\uparrow}$, $E_{\text{Néel}} = -23.58E_{\uparrow\uparrow}$, i.e., $E_{\text{vortex}}^{\text{forced}} > E_{\text{Néel}}$. As it is not possible to assign a direction to a quadrupole, we do not compare the energy to the forced pinwheel state but the $s=0.8$ state (see below). Forcing the moments into this structure results in an energy of $E_{s=0.8\ \text{state}}^{\text{forced}} = -19.07E_{\uparrow\uparrow}$. Hence, the 120° Néel state for $s=0.45$ has a significantly lower energy than the pure dipole or pure quadrupole structures. However, in the latter case the energy per particle increases only by $0.38E_{\uparrow\uparrow}$, while it is $1.8E_{\uparrow\uparrow}$ for the vortex state.

If $s$ exceeds 0.45 the 120° Néel state disappears and out-of-plane components emerge. At $s=0.8$ the pinwheel state[6] has formed. However, in this small cluster the pinwheel state

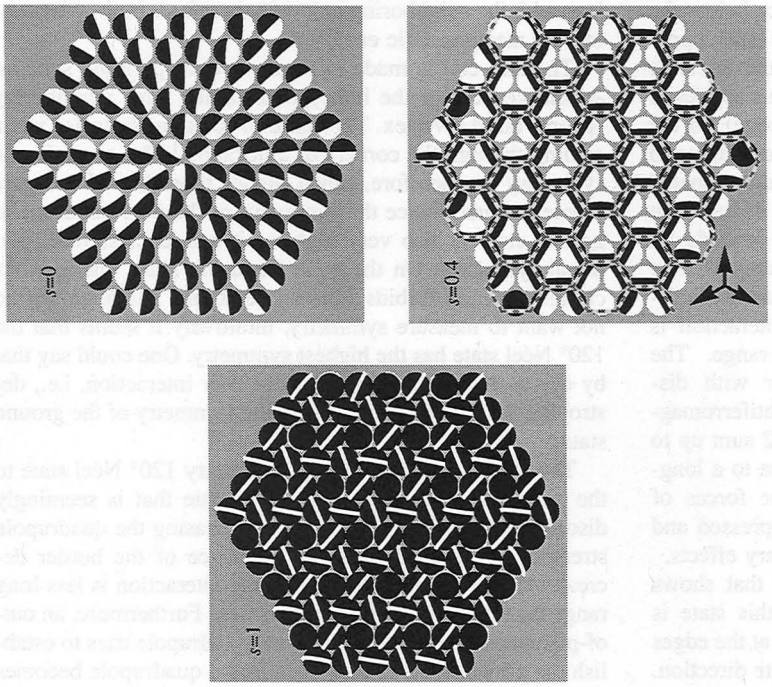


FIG. 7. (Color online) Monte Carlo simulation of 108-particle clusters. In case of $s=0$ each sextant shows a collinear state, which is, therefore, called quasiferromagnetic. For $s=0.4$ almost the full area shows the 120° Néel state but at the edges some weakly bound spheres have deviating orientations. The three arrows in the lower right corner schematically show the high symmetry of the unit cell. Choosing this unit cell, the cell boundaries are given by the honeycomb lattice drawn on top of the simulated structure (dashed line). At $s=1$ the pinwheel state forms, for which—as in Fig. 6—only the equatorial plane is drawn.

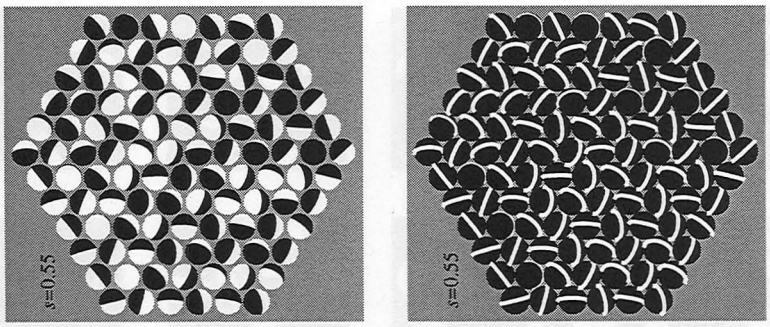


FIG. 8. Monte Carlo simulation of 108-particle clusters with $s=0.55$. In the left graph the state is shown using the standard representation of capped spheres, while in the right graph the orientation of the dipole is neglected, i.e., only the orientation of the quadrupole is shown via the white line of the sphere's equatorial plane. While the left graph seems rather disordered the right one shows domains of a pinwheel state coexisting with herringbone structure domains.

of the quadrupole ($s=1$) differs from the state formed in case of $s=0.8$. In the latter case the small dipole moment contribution still prefers a vortex flux closure. Note that the symmetry of the triangle, formed by the pinwheel centers (Fig. 6, $s=0.8$), is consistent with the cluster symmetry. This symmetry allows the formation of three vortices coupling via an additional vortex in the center. For the pure quadrupole the triangle, formed by the pinwheel centers, is rotated by $\pi/6$. This position allows a complete pinwheel in the lower part of the cluster (Fig. 6, $s=1.0$). However, this difference is only a size effect and vanishes with increasing cluster size due to frustration, i.e., in large systems it is geometrically impossible to form a perfect dipole vortex at every pinwheel at the same time.

Obviously, the 120° Néel state only appears in a small region of $0.35 \lesssim s \lesssim 0.5$, i.e., where dipole-dipole- and quadrupole-quadrupole-interaction energies are almost equal. The borders of this region might change with cluster size and due to the influence of higher-order moments. However, for the investigated clusters the size has an influence below the presented resolution of $\Delta s=0.05$. The lower and upper boundaries of the 120° Néel state are within the intervals $0.35<s<0.4$ and $0.45<s<0.5$, respectively. This applies to the edge-dominated 12-particle clusters (75% edge), to the 27-particle clusters with almost equal amount of edge and center spheres (55%/45%), as well as to the area dominated 108-particle clusters (70% area). From this we deduce that the parameter space of stability only weakly depends on cluster size even for larger clusters. This can be supported by the following consideration. Due to the local quasiantiferromagnetic order the long-range dipole-dipole interaction is suppressed, which then only acts at short range. The quadrupole-quadrupole interactions drop faster with distance. Additionally, in one unit cell with quasiantiferromagnetic order all quadrupole moments with $m=\pm 2$ sum up to zero.[24] The nonvanishing $Q_{20}$ does not contribute to a long-range dipole-quadrupole interaction. Hence, the forces of long-range interactions on the structure are suppressed and finite-size effects are basically only local boundary effects.

On the other hand, the narrow region of $s$ that shows stability of the 120° Néel state suggests that this state is sensitive to perturbations. Weakly bound spheres at the edges of a cluster may easily point in a non-ground-state direction. This is observed experimentally[1] as well as in all simulations with cluster of 27 particles or larger. An example demonstrating this behavior is shown in the upper right graph of Fig. 7. For $s=0.40$ the 120° Néel state has formed on a 108-particle cluster. As for large clusters it is likely (83%) that the 120° Néel state does not freeze symmetrically with respect to the cluster shape; some edge particles even point in the $z$ direction.

The 120° Néel state is a superstructure on the triangular lattice that has the full symmetry of a triangle itself. To emphasize the high symmetry, the honeycomb lattice is added (Fig. 7). Note that in a simple picture of point charges, pure dipoles ($\oplus$—$\ominus$) would introduce three negative charges in the center of the unit cell. The point-charge representation of the quadrupole has the form ($\oplus -2\times \ominus -\oplus$). Combining dipole and quadrupole with $s=0.4$ results in a point-charge distribution (inside-out) ($\frac{1}{5}\times \ominus -\frac{4}{5}\times \ominus -1\times \oplus$). Hence, the center charge that would strongly increase the energy is decreased. Additionally, the "ring" of the outer charges overlaps with the neighboring unit cell, therefore, further decreasing the magnetostatic energy.

The unit cell is made of three outward pointing spheres. At the vertices of the honeycomb lattice three neighboring spheres build a vortex. The sense of rotation alternates when cycling through the corners of a hexagon.[1] The ground-state symmetry is, therefore, much higher than that of the pure dipole. At first glance the symmetry of the pure quadrupolar ground state is also very high, as it has, e.g., sixfold rotational symmetry. On the other hand the latter one exhibits chirality, which forbids mirror operations. Although we do not want to measure symmetry, intuitively it seems that the 120° Néel state has the highest symmetry. One could say that by decreasing the symmetry of the pair interaction, i.e., destroying the parity, one increases the symmetry of the ground state.

The transition from the high symmetry 120° Néel state to the pinwheel state is realized via a state that is seemingly disordered (see Fig. 8, left): when increasing the quadrupole strength, i.e., increasing $s$, the influence of the border decreases as the quadrupole-quadrupole interaction is less long range than the dipole-dipole interaction. Furthermore, an out-of-plane component emerges as the quadrupole tries to establish the pinwheel state. However, as the quadrupole becomes

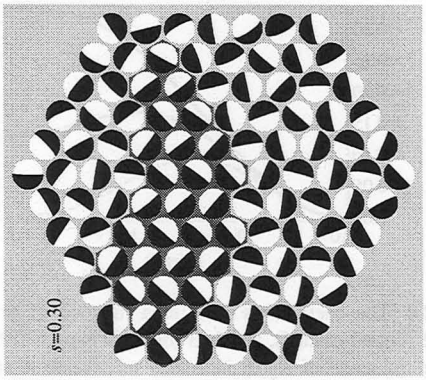


FIG. 9. (Color online) Monte Carlo simulation for a 108-particle cluster with $s=0.3$. The cluster shows several domains with a herringbone structure. The largest domain is highlighted.

the dominating part, it is already interesting to look at the ordering of the quadrupole moments or in other words to forget about the sign of the dipole. To do so one can use the representation of quadrupoles used in the last graph of Fig. 6 even in the case of a non-negligible dipole moment. This representation is realized in the right graph of Fig. 8. Some pinwheels have formed in the upper right and lower left, while the center and lower right form a herringbone structure. As shown above for 12-particle clusters the energy per particle with $s=0.45$ is only slightly higher when forced from a 120° Néel onto a pinwheel state. Obviously at $s=0.55$ the transition to the pinwheels state, where 25% of the particles have an out-of-plane component (pinwheel axis), takes place. Additionally, the directional order of the dipole is gradually lost. As the dipole is sensitive to the presence of edges there is a difference between center and rim. Hence, the transition state depends on cluster size.

When on the other hand the dipole is increased, the interaction becomes more long range and the system has to change from a quasiantiferromagnetic to a quasiferromagnetic state (see Fig. 7): in this situation the compromise between collinear and noncollinear states is a herringbone structure (see Fig. 9). As mentioned before, this structure is rather typical for quadrupoles on a hexagonal lattice. According to the pole avoidance principle, on every finite cluster the dipole eventually forces a flux closure and, consequently, the herringbone structure cannot be monodomain but the domain size will depend on cluster size. Hence, the occurrence and the size of these domains are also a property depending on system size.

In contrast to this, the states with a long-range order, i.e., the vortex of pure dipoles, the pinwheel state of pure quadrupoles, and of course the 120° Néel state at $s\approx 0.4$, are well characterized even by small clusters like the ones presented in Fig. 6. Hence, finite-size effects are important when investigating phase transitions, critical exponents, domains, and domain walls, while typical ground-state symmetries can already form for very small clusters. As the simulations are supposed to describe the experiment presented in Ref. 1, where the clusters are rather small as well as gradually constructed, which suppresses domain formation, very large clusters and domain formation are not discussed here.

Finally, the question arises to what extent the decision to neglect higher-order multipole moments is justified. The analytical calculations give a small positive octopole moment. The calculated quadrupole moment, however, is smaller than the one required to form the 120° Néel state. The smaller quadrupole would probably require a negative octopole that reduces the dipole's tendency toward a collinear state and, therefore, to re-establish the 120° Néel state. A negative octopole moment is not expected from a dipole layer shifted in the positive $z$ direction. Furthermore, only the dipole-octopole interaction would decrease the stability of the collinear state, while the octopole-octopole interaction favors a collinear state as well. Beyond these considerations of plausibility we assume that the 120° Néel state is easily affected by higher-order moments and that nonzero higher-order moments should be small compared to the quadrupole. Hence, the interaction of the spheres cannot be modeled by an off-center dipole inside the sphere as proposed earlier.[1] When shifting a dipole off center, higher-order moments emerge. If a dipole of the form $Q_{10}$ is shifted in the $z$ direction, i.e., the coordinate system in $-z$, and utilizing Eq. (4), a quadrupole $Q_{20}=2Q_{10}z$, an octopole $Q_{30}=3Q_{10}z^2$, and higher orders appear. As the spheres are separated by one unit distance, the sphere radius is $\hat{u}/2$. To get a quadrupole similar to $s=0.4$, the dipole must be shifted by $z=\hat{u}/3$, making the dipole-dipole and the quadrupole-quadrupole energies identical. Note that the dipole would still be inside the sphere. However, the emerging octopole would result in an octopole-octopole energy that would be 70% of the dipole-dipole energy. Hence, the octopole would significantly change the energy and the ground state, as both, dipole and octopole, prefer a collinear state. The detailed influence of higher-order moments, especially the octopole, is part of ongoing investigations.

## V. SUMMARY

It has been shown that hemispherical radially magnetized caps have multipole moments beyond the dipole. A radially magnetized hemisphere with constant capping thickness and constant surface charge would have a potential with inversion symmetry, i.e., a hemisphere with magnetic material on the opposite side has the same magnetic potential. This cannot explain the experimental results. If, on the other hand, the magnetization or the magnetic surface charge decreases toward the edge of the cap or the cap is magnetic only up to a critical angle $\theta_c$ a quadrupole moment emerges. The quadrupole moment is the first and most important correction term to the typical dipole approximation. The quadrupole's even parity is required to destroy the inversion symmetry, ensuring that upon rotation of the spheres—interchanging capped and noncapped hemispheres—the energy changes. As the presented model for the magnetic cap is an oversimplification, it has not been used to extract quantitative values for the quadrupole moment. In lieu thereof the mixing from dipole and quadrupole was evaluated from the pure dipole to the pure quadrupole and for magic cluster sizes up to 108 particles.

The 120° Néel state observed in experiment is stable only in a small region of mixing ratios where dipole-dipole and

quadrupole-quadrupole interactions are comparable. Assuming that moments beyond the quadrupole are negligible, it has been possible to estimate the relative strength of the quadrupole moment—compared to the dipole—from the cap orientations in a three-particle cluster. The result is in good agreement with the required strength of the quadrupole moment to form the 120° Néel state in larger clusters.


## ACKNOWLEDGMENTS

The support by the Deutsche Forschungsgemeinschaft in the framework of SFB 668, subproject A11, and IRTG Soft Condensed Matter is acknowledged.


## APPENDIX: THE COEFFICIENTS $A_l$

To calculate the coefficients $A_l(\theta)$ one starts with integrating Eq. (2) over the cap surface, including a charge density varying with $\cos\theta$. When the integration stops at $\theta$ the coefficients have the form

$$A_l(\theta) = \frac{P_{l-2}(\cos\theta) - P_l(\cos\theta)}{(2l-1)(2l+1)} + \frac{\cos\theta[P_{l-1}(\cos\theta) - P_{l+1}(\cos\theta)]}{2l+1} - \frac{P_l(\cos\theta) - P_{l+2}(\cos\theta)}{(2l+3)(2l+1)}, \quad \text{(A1)}$$

where $P_l$ is the Legendre polynomial of order $l$. If $\theta = \pi/2$ Eq. (A1) simplifies to

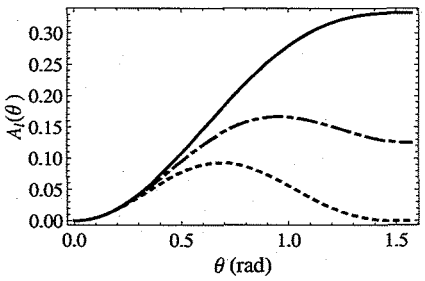


FIG. 10. The coefficients $A_l(\theta)$ as a function of $\theta$: $l=1$ (solid line), $l=2$ (dotted dashed), and $l=3$ (dotted). Note that for decreasing $\theta$ the influence of $A_2(\theta)$ increases relative to $A_1(\theta)$, i.e., the quadrupole becomes more important.

$$A_l\left(\frac{\pi}{2}\right) = \begin{cases} \dfrac{1}{3}, & l=1 \\ \dfrac{1+(-1)^l}{8\sqrt{\pi}}(-1)^{l/2+1}\dfrac{\Gamma\frac{l-1}{2}}{\Gamma\frac{l+4}{2}}, & l>1. \end{cases} \quad \text{(A2)}$$

The first factor is only nonzero if $l$ is even. Hence, for $\theta = \pi/2$ the only odd moment is the dipole moment. All higher-order moments are even. The main correction to the dipole is given by the second order, the quadrupole moment. If $\theta$ differs from $\pi/2$ additional odd moments—like the octopole in Fig. 10—emerge but are negligible for $\theta > \pi/3$.


*nmikusze@physnet.uni-hamburg.de



[1] L. Baraban, D. Makarov, M. Albrecht, N. Rivier, P. Leiderer, and A. Erbe, Phys. Rev. E **77**, 031407 (2008).

[2] E. Y. Vedmedenko, *Competing Interactions and Pattern Formation in Nanoworld* (Wiley-VHC, Weinheim, 2007).

[3] A. Brooks Harris, Phys. Rev. B **2**, 3495 (1970)

[4] M. J. Mandell, J. Chem. Phys. **60**, 1432 (1974).

[5] M. J. Mandell, J. Chem. Phys. **60**, 4880 (1974).

[6] A. J. Berlinsky and A. B. Harris, Phys. Rev. Lett. **40**, 1579 (1978).

[7] K. De'Bell, A. B. MacIsaac, I. N. Booth, and J. P. Whitehead, Phys. Rev. B **55**, 15108 (1997).

[8] E. Y. Vedmedenko, A. Ghazali, and J.-C. S. Lévy, Phys. Rev. B **59**, 3329 (1999).

[9] M. Eremtchenko, J. A. Schaefer, and F. S. Tautz, Nature (London) **425**, 602 (2003).

[10] J. D. Jackson, *Classical Electrodynamics* (Wiley, New York, 1962).

[11] J. Kongsted, A. Osteda, K. V. Mikkelsena, and O. Christiansen, Chem. Phys. Lett. **364**, 379 (2002).

[12] S. G. Kukolich and W. H. Flygare, Mol. Phys. **17**, 127 (1969).

[13] V. E. Klymenko, V. M. Rozenbaum, V. V. Kukhtin, and O. V. Schramko, Solid State Commun. **88**, 373 (1993).

[14] A. S. Clarke and G. N. Patey, J. Chem. Phys. **100**, 2213 (1994).

[15] H. J. Nam, D.-Y. Jung, G.-R. Yi, and H. Choi, Langmuir **22**, 7358 (2006).

[16] M. Albrecht, G. Hu, I. L. Guhr, T. C. Ulbrich, J. Boneberg, P. Leiderer, and G. Schatz, Nature Mater. **4**, 203 (2005).

[17] A. Ashkin, J. M. Dziedzic, J. E. Bjorkholm, and S. Chu, Opt. Lett. **11**, 288 (1986).

[18] A cluster is called magic if its outer shell is closed. This is the case if it contains $n=3k^2$, $k \in \mathbb{N}$ particles (Ref. 1).

[19] B. Bernu, P. Lecheminant, C. Lhuillier, and L. Pierre, Phys. Rev. B **50**, 10048 (1994).

[20] A. J. Stone, *The Theory of Intermolecular Forces* (Clarendon, Oxford, 1996).

[21] T. C. Ulbrich, D. Makarov, G. Hu, I. L. Guhr, D. Suess, T. Schrefl, and M. Albrecht, Phys. Rev. Lett. **96**, 077202 (2006).

[22] D. A. Varsalovich, A. N. Moskalev, and V. K. Khersonskii, *Quantum Theory of Angular Momentum* (World Scientific, Singapore, 1988).

[23] E. Y. Vedmedenko, N. Mikuszeit, H. P. Oepen, and R. Wiesendanger, Phys. Rev. Lett. **95**, 207202 (2005).

[24] Note that when rotating an axial quadrupole (pointing in the $z$ direction) by $\pi/2$ around $y$ to in plane, moments with $m=\pm 2$ emerge.